ORIGINAL ARTICLE

Journal Section

Solving Singular Control Problems using Uniform Trigonometrization Method

Kshitij Mall[1*] | **Ehsan Taheri**[1*] | **Prathamesh Prabhu**[2†]

[1]Department of Aerospace Engineering, Auburn University, Auburn, AL, 36849

[2]School of Chemical Engineering, Purdue University, West Lafayette, IN, 47907

Correspondence
Kshitij Mall, Department of Aerospace Engineering, Auburn University, Auburn, AL, 36849
Email: mall@auburn.edu

Funding information
This work was not funded by any agency.

This study investigates the application of a recently developed construct, the Uniform Trigonometrization Method (UTM), to the singular control problems in chemical engineering. The UTM involves minimal modifications to the original problem, thereby generating near-singular control solutions that can be used for conceptual design and serve as an alternate to direct techniques like nested and simultaneous approaches. Eight classical singular control problems with known analytical solutions and three complex singular control problems from chemical engineering domain are solved in this study. The results obtained using the UTM for these problems are found to match well with the literature and are of higher resolution as compared to the results obtained using a direct pseudospectral based solver. The ability of the UTM to handle complex chemical engineering problems with both singular controls and state path constraints has also been demonstrated in this study.

KEYWORDS
Singular Control, Trigonometric Functions, Indirect Optimization Method, Batch Plant Designs, Distillation, Reactor Analysis

1 | INTRODUCTION

OPTIMIZATION is important for process modeling, process equipment designing, optimum economic operations, synthesis and retrofitting of chemical, petrochemical, pharmaceutical, energy and related processes [1]. In industry, chemical engineers optimize the process operation and design usually for improving the performance, cost,

sustainability, reliability and safety of systems [1, 2]. In the field of chemical engineering, the major application is minimizing the energy consumption [2]. All the aforementioned factors eventually affect the estimation of the overall cost for any plant design [2].

Singular control plays a vital role in process engineering, including optimal operation of batch and semi-batch reactions [3, 4, 5]. The singular control could be mainly in the form of catalyst distribution along the reactor [6] or temperature profile of the reactor with the ultimate goal of maximizing the product yield without investing capital [7]. Singular control problems have various applications ranging from optimization of reactors, i.e., plug flow reactors [8, 9], stirred tank reactors [10], and tubular reactors [9] to optimization of distillation columns [11], from batch processes [12] to semi-batch processes [13], from singular bed problems to multiple-bed problems [14]. However, for several practical applications, accurate solution of singular control profiles is still not resolved, in particular, for processes with highly non-linear dynamics.

Computational methods for solving optimal control problems (OCPs) can be classified as *direct* methods and *indirect* methods, where the solution is sought by various iteration procedures [15]. Singular control problems have very few computational methods due to the complexity in programming. Pseudospectral methods (PSMs) are popular direct methods that can simultaneously solve OCPs comprising control and state path constraints. However, the PSMs yield jittery control solutions while solving singular control problems, which is shown later in this study. A nested direct transcription optimization method [16] was devised by Chen and Biegler in which inner and outer problems need to be solved to obtain singular controls. In this nested approach, the discretized Euler-Lagrange equations [17] of the singular control problem are satisfied. The nested approach was found to be computationally slow due to the complexity involved in its algorithm.

Chen and Biegler improved upon the nested optimization method and devised a more efficient simultaneous approach [18], which includes a heuristic approach for the outer problem of the nested approach. The simultaneous approach comprises three stages: stage 1 comprises coarse distribution of finite elements with sufficiently many finite elements over instances with steep control profiles and insertion of fixed grid points based on errors in state profiles. Stage 2 inserts moving grid points where the modified switching conditions are violated to yield an initial solution. In stage 3, accuracy of the switching points is improved by spike removal, switching point detection, and moving grid updates until the modified switching conditions are satisfied. The simultaneous approach, although very accurate and computationally fast, requires users to implement the complicated algorithm involved. Furthermore, the simultaneous approach is devoid of more insightful, analytical expressions for the control law.

Silva and Trélat [19] developed an indirect smoothing technique based on polynomial functions to regularize singular control problems and to obtain unique singular control law for such problems. To improve upon the smoothing technique, Mall and Grant [20, 21] devised the Epsilon-Trig Regularization Method (ETRM) using trigonometric functions in the indirect formalism. The principal idea in Refs. [19, 20, 21] is to regularize the problem by introducing small error parameters and error-control terms. Mall et al. recently presented a new technique, named as Uniform Trigonometrization Method (UTM), with the ability to solve various types of OCPs with control and state constraints using an indirect methodology [22, 23]. The UTM is more advanced than the ETRM and requires minimal changes to the original problem formulation. PSM was found deficient in solving the complicated problem of maximizing energy obtained from the waves in Ref. [24], whereas UTM yielded high-quality solution for the same. The UTM has also been employed in solving complicated problems from the atmospheric flight mechanics domain [22, 25]. The UTM can thus be considered as an alternative for existing numerical methods like the simultaneous approach used to obtain singular control solutions for OCPs.

The first contribution of this study is showcasing the ability of the UTM in solving complicated singular control problems in the chemical engineering domain. The UTM utilizes built-in functions *ode45* and *bvp4c* of MATLAB, which

makes the UTM accessible to a broader range of users due to the availability of such tools to the scientific community. The second contribution made by this study is solving singular control problems that are subject to state path constraints in a simultaneous manner using the UTM. The presence of state path constraints is a challenge to the application of indirect optimization methods, but the UTM is capable of handling such constraints that may arise in formulating chemical engineering problems in realistic settings.

The remaining sections of this article are organized as follows. Section 2 contains a brief description about the singular control problems and the traditional indirect approach for solving such problems. Section 3 presents the recently developed UTM construct that can efficiently solve singular control problems and OCPs with state path constraints. Section 4 showcases the application of the UTM to 11 singular control problems including three complex chemical engineering problems. The results obtained using the UTM for these problems are compared with the corresponding solutions obtained using the PSM and the literature. This study is concluded in Section 5.

2 | PRELIMINARIES

2.1 | Formulation of Optimal Control Problems

Let $\boldsymbol{x} \in \mathbb{R}^n$ and $\boldsymbol{u} \in \mathbb{R}^m$ denote the state and control vectors, respectively. The cost functional, J, for a standard OCP can be written in Bolza form as

$$J = \phi(\boldsymbol{x}(t_f), t_f, \boldsymbol{x}(t_0), t_0) + \int_{t_0}^{t_f} L(\boldsymbol{x}(t), \boldsymbol{u}(t), t)dt, \tag{1}$$

where ϕ is the scalar terminal cost, L is the path cost, t_0 and t_f denote the initial and final limits of time, respectively. The cost functional is subject to a number of constraints usually written as

$$\text{Differential equations: } \dot{\boldsymbol{x}}(t) = \boldsymbol{f}(\boldsymbol{x}(t), \boldsymbol{u}(t), t), \tag{2a}$$

$$\text{Boundary constraints: } \boldsymbol{\Psi}(\boldsymbol{x}(t_f), t_f, \boldsymbol{x}(t_0), t_0) = \boldsymbol{0}, \tag{2b}$$

$$\text{State path constraints: } \boldsymbol{x}_{\text{MIN}} \leq \boldsymbol{x}(t) \leq \boldsymbol{x}_{\text{MAX}}, \tag{2c}$$

$$\text{Control constraints: } \boldsymbol{u}_{\text{MIN}} \leq \boldsymbol{u}(t) \leq \boldsymbol{u}_{\text{MAX}}, \tag{2d}$$

where $\boldsymbol{x}_{\text{MIN}}$, $\boldsymbol{x}_{\text{MAX}}$, $\boldsymbol{u}_{\text{MIN}}$, and $\boldsymbol{u}_{\text{MAX}}$ denote the specified lower and upper bounds for the states and controls, respectively. Also, $\boldsymbol{\Psi} \in \mathbb{R}^p$ for $p < n$. The differential equations of motion play the role of constraints between the time derivative of the states and a vector-valued function space at any time instance along the trajectory.

2.2 | First-Order Necessary Conditions of Optimality

A brief review of first-order necessary conditions of optimality is given since these conditions are extensively used in this paper. A mathematical quantity called the Hamiltonian simplifies the derivation of the necessary conditions of optimality and is defined as

$$H = L(\boldsymbol{x}, \boldsymbol{u}, t) + \boldsymbol{\lambda}^T \boldsymbol{f}(\boldsymbol{x}, \boldsymbol{u}, t), \tag{3}$$

where $\boldsymbol{\lambda} \in \mathbb{R}^n$ is the costate vector associated with the state vector. Costates have their corresponding dynamics, which are obtained through Euler-Lagrange equations given as

$$\dot{\boldsymbol{\lambda}} = -\left[\frac{\partial H}{\partial \boldsymbol{x}}\right]^T. \tag{4}$$

Let $\Phi = \phi + \boldsymbol{\nu}^T \boldsymbol{\Psi}$ where $\boldsymbol{\nu} \in \mathbb{R}^p$ denote the vector of constant Lagrange multipliers, which are used to adjoin the boundary conditions to the cost functional. Equation (5a) shows the optimal control law, $\boldsymbol{u}(t)$, as a function of the states and costates, which is also known as the strong form of optimal control. Equations (5b) and (5c) specify the initial and terminal boundary conditions on the costates, collectively known as the transversality conditions. It is possible for the final time, t_f, to be a parameter that has to be optimized. The free final time condition, shown by Eqs. (5d) and (5e), define conditions that have to be taken into account for free-final-time problems. These equations are known as the stationary conditions. Equations (4)–(5e) form a well-defined TPBVP and define the set of first-order necessary conditions of optimality, which any extremal solution to the cost functional has to satisfy. BVP solvers such as MATLAB's *bvp4c* can solve such a TPBVP.

$$\frac{\partial H}{\partial \boldsymbol{u}} = 0, \tag{5a}$$

$$\boldsymbol{\lambda}(t_0)^T + \frac{\partial \Phi}{\partial \boldsymbol{x}(t_0)} = \boldsymbol{0}, \tag{5b}$$

$$\boldsymbol{\lambda}(t_f)^T - \frac{\partial \Phi}{\partial \boldsymbol{x}(t_f)} = \boldsymbol{0}, \tag{5c}$$

$$\left(H + \frac{\partial \Phi}{\partial t}\right)_{t=t_f} = 0, \tag{5d}$$

$$\left(H - \frac{\partial \Phi}{\partial t}\right)_{t=t_0} = 0. \tag{5e}$$

Equation (5a) applies to problems in which the control is unbounded and the Hamiltonian is a non-linear function of the control input. There are cases that the strong form of optimality does not apply. When more than one option exists after solving Eq. (5a), PMP helps select the optimal control as shown in Eq. (6), where superscript '*' refers to the optimal value [17]. It states that the optimal control will minimize the Hamiltonian, H, for all admissible values of control [17]. For all OCPs in this paper, it is assumed that $t_0 = 0$ s and is fixed.

$$H(t, \boldsymbol{x}^*(t), \boldsymbol{u}^*(t), \boldsymbol{\lambda}^*(t)) \leq H(t, \boldsymbol{x}^*(t), \boldsymbol{u}(t), \boldsymbol{\lambda}^*(t)). \tag{6}$$

2.3 | Bang-Bang Control and Singular Arcs

Suppose a bounded OCP with a scalar control, u, has a Hamiltonian, H, as shown in Eq. (7) [17]. The control is allowed to take values between its admissible lower and upper limits denoted by u_{MIN} and u_{MAX}, respectively. Since H is linear in u, Eq. (5a) results in Eq. (8).

$$H = H_0(t, \boldsymbol{x}(t), \boldsymbol{\lambda}(t)) + H_1(t, \boldsymbol{x}(t), \boldsymbol{\lambda}(t))u, \tag{7}$$

$$\frac{\partial H}{\partial u} = H_1. \tag{8}$$

In Eq. (7) the Hamiltonian is written as two terms: 1) H_0 that denotes the collection of all terms that does not depend on control input and 2) H_1 that denotes a coefficient multiplied with the control input. The choice of u cannot influence $H_0(t, \boldsymbol{x}^*(t), \boldsymbol{\lambda}(t))$, so the solution process ignores this term. If H_1 is positive, then the solution process should take the lowest value of u to minimize H according to the PMP. Similarly, if H_1 is non-positive, the process should take the maximum value of u. In summary, the PMP gives the control law as

$$u^* = \begin{cases} u_{\text{MIN}}, & \text{if } H_1 > 0, \\ \in [u_{\text{MIN}}, u_{\text{MAX}}], & \text{if } H_1 = 0, \\ u_{\text{MAX}}, & \text{if } H_1 < 0. \end{cases} \tag{9}$$

The coefficient $H_1(t, \boldsymbol{x}^*(t), \boldsymbol{\lambda}(t))$ is known as the switching function. When H_1 alternates between positive and negative values, the control law switches back and forth between its lower and upper bounds, attaining a profile known as "bang-bang". When $H_1 \equiv 0$ during one (or multiple) non-zero time interval(s), say $t_0 \leq t_1 < t_2 \leq t_f$, then the subarc $[t_1, t_2]$ is characterized as a singular subarc and the control no longer influences H, leading to non-uniqueness issues. To determine unique candidate singular controls, the traditional approach differentiates Eq. (5a) with respect to time as shown in Eq. (10). The last term in Eq. (10) vanishes because the derivative of the Hamiltonian with respect to the control, H_u, does not contain u and $\frac{\partial H_u}{\partial u}$ becomes 0 as a result.

$$\dot{H}_u = 0 = \frac{\partial H_u}{\partial t} + \left[\frac{\partial H_u}{\partial \boldsymbol{x}}\right]^T \dot{\boldsymbol{x}} + \left[\frac{\partial H_u}{\partial \boldsymbol{\lambda}}\right]^T \dot{\boldsymbol{\lambda}} + \left[\frac{\partial H_u}{\partial \boldsymbol{u}}\right]^T \dot{\boldsymbol{u}}. \tag{10}$$

The solution process forms $\frac{d^2}{dt^2} H_u \equiv 0$, and if u appears explicitly, the process uses the condition specified in Eq. (10) along with the Kelley's condition, which is given as

$$(-1)^q \frac{\partial}{\partial u}\left(\frac{d^{2q} H_u^*}{dt^{2q}}\right) \geq 0, \tag{11}$$

to determine the singular control law. If u does not appear explicitly, the solution process takes even time derivatives of H_u until the process satisfies Kelley's condition along with the conditions specified by odd time-derivatives of H_u [17] to obtain the singular control law. For certain singular control problems, the value of q may become very large, leading to longer problem formulation and problem solving times. In addition, for problems with complex non-linear dynamics, the resulting algebraic expressions can become lengthy and hard to derive.

The OCPs involving state path constraints require solving a multi-point boundary value problem (MPBVP), which is very complicated to solve and formulate. Furthermore, *a priori* information about the location and the sequence of the constraint arcs is required to formulate and solve the state constraint problems [26].

3 | UNIFORM TRIGONOMETRIZATION METHOD

Instead of solving singular control problems in a tedious manner using Kelley's condition or solving a complicated MPBVP for incorporating path constraints while using traditional indirect methods, a much simpler technique could be adopted to simultaneously solve for several control and state path constraints. This section contains a brief description of the simpler methodology based on trigonometric functions, dubbed as the UTM, for solving singular control problems along with state path constraints [22]. The UTM also has the ability to solve OCPs with control constraints upon

non-linear controls, which is excluded from discussion in this section for brevity.

Consider a general OCP comprising m linear controls with constraints of the form $u_{i_{\text{MIN}}} \leq u_i \leq u_{i_{\text{MAX}}}$ (for $i \in \{1, \ldots, m\}$) and n along-the-path state constraints of the form $S_{j_{\text{MIN}}} \leq S_j \leq S_{j_{\text{MAX}}}$ (for $j \in \{1, \ldots, n\}$). For simplicity of discussion, it is assumed that each control appears in only one state dynamics.

All indirect optimization methods ultimately require minimizing (or maximizing) the Hamiltonian, which is written for the given control and state constraints as

$$H = H_0(t, \boldsymbol{x}, \boldsymbol{\lambda}) + \sum_{i=1}^{m} H_{1_i}(t, \boldsymbol{x}, \boldsymbol{\lambda}) u_i, \tag{12}$$

where H_0 denotes set of terms that are independent of control inputs; H_{1_i} denotes the switching function corresponding to the i-th control input. The OCP can then be described as

$$\text{minimize } \tilde{J} = \phi(\boldsymbol{x}(t_f), t_f, \boldsymbol{x}(t_0), t_0) + \int_{t_0}^{t_f} \tilde{L}(\boldsymbol{x}, \boldsymbol{u}, t)\, \mathrm{d}t, \tag{13a}$$

$$\text{subject to } \dot{\boldsymbol{x}}_i = f_i(t, \boldsymbol{x}) + g_i(t, \boldsymbol{x}) u_i, \tag{13b}$$

$$\text{where } \tilde{L} = L + \sum_{i=1}^{m} \epsilon_i \cos u_{i_{\text{TRIG}}} + \sum_{j=1}^{n} \epsilon_j \sec\left(\frac{\pi}{2}\left(\frac{2S_j - S_{j_{\text{MAX}}} - S_{j_{\text{MIN}}}}{S_{j_{\text{MAX}}} - S_{j_{\text{MIN}}}}\right)\right), \tag{13c}$$

where $\tilde{J}$ is the modified cost functional; the state EOMs, comprising the bounded controls, are shown in Eq. (13c). $\tilde{L}$ consists of the terms $\epsilon_i \cos u_{i_{\text{TRIG}}}$ that account for regularizing m bang-bang and singular controls, where ϵ_i is an error parameter and $\cos u_{i_{\text{TRIG}}}$ is an error control corresponding to the i-th control. The secant terms in $\tilde{L}$ act as penalties for violation of the n state constraints, S_j, where ϵ_j is the error parameter corresponding to the j-th state constraint. For dimensional consistency, ϵ_i has units equal to $\dfrac{\text{units of } L}{\text{units of } u_i}$ while ϵ_k has the same units as L.

All bounded linear controls, u_i, are specified in trigonometric forms in the UTM as

$$u_i = c_{1_i} \sin u_{i_{\text{TRIG}}} + c_{0_i}, \tag{14a}$$

$$\text{where } c_{0_i} = \frac{u_{i_{\text{MAX}}} + u_{i_{\text{MIN}}}}{2}, \quad c_{1_i} = \frac{u_{i_{\text{MAX}}} - u_{i_{\text{MIN}}}}{2}. \tag{14b}$$

Observe that u_i is substituted in the right-hand side of Eq. (13b). Thus, u_i is mapped into $u_{i_{\text{TRIG}}}$, which is the argument of the sine term. Using Eqs. (5a), (12), and (14), the strong form of optimality can be written for this regularized problem as

$$\frac{\partial H}{\partial u_{i_{\text{TRIG}}}} = -\epsilon_i \sin u_{i_{\text{TRIG}}} + c_{1_i} H_{1_i} \cos u_{i_{\text{TRIG}}} = 0 \quad \forall \quad i \in \{1, \cdots, m\}. \tag{15}$$

Since the Hamiltonian is now a non-linear function of control inputs, the optimal control options for the m bang-bang and singular controls are thereby obtained using Eq. (15) and are shown as

$$u^*_{i_{\text{TRIG}}} = \begin{cases} \arctan\left(\dfrac{c_{1_i} H_{1_i}}{\epsilon_i}\right), \\ \arctan\left(\dfrac{c_{1_i} H_{1_i}}{\epsilon_i}\right) + \pi, \end{cases} \tag{16}$$

where H_{1_i} is the switching function for the i-th control input (for $i = 1, \cdots, m$). During the numerical simulations, at each time instant, PMP is used to select the optimal control from among the options listed in Eq. (16). The use of

trigonometric functions along with a minuscule error in the UTM enables generating a closed-form, analytical expression for the near-singular control law, which is more insightful. The secant terms in Eq. (4) result in modified costate dynamics obtained using Eq. (13a).

As a consequence of applying the above mappings, the structure of the original problem is altered using the UTM. The original, difficult-to-solve OCP is transformed into a many-parameter family of neighboring OCPs. Thus, in order to recover the solution for the original OCP, the value of ϵ_i has to be exactly 0. However, near-zero values are sufficient to obtain a solution that is nearly optimal for all engineering problems [27]. Numerical issues will arise if ϵ_i has an exact 0 value, which is therefore avoided without sacrificing optimality. Note that the UTM uses different ϵ for different control and state constraints; each ϵ has units, which ensures dimensional consistency. In the literature, ϵ is usually considered as a dimensionless parameter, which could lead to dimensional inconsistency issues.

The differences between the approaches mentioned in this study to solve the singular control problems are summarized in Table 1. Note that the accuracy of the PSM is described as variable because many times the singular solutions obtained using the PSM are very close to the actual solutions, but many other times the control solutions are quite jittery. Table 1 also shows that all the four methods have their own pros and cons, but overall the UTM is a good alternate. Solving same problem using different existing methods also helps in gaining enough confidence about the optimality of the solutions.

TABLE 1 Comparison between different approaches to solve singular control problems.

Attribute	PSM [28]	Nested Approach [16]	Simultaneous Approach [18]	UTM [22]
Type	Direct	Direct	Direct	Indirect
Accuracy	Variable	High	Very High	High
Computation Time	Small	Large	Very Small	Medium
Incorporate Path Constraints	Yes	No	No	Yes

4 | NUMERICAL RESULTS

Eight benchmark examples with known analytical solutions and three complex problems from chemical engineering domain [16, 18] are solved using the UTM in the following sub-sections. A comparison is drawn between the solutions obtained using the UTM and the PSM. Default setup of GPOPS-II [28] was used along with a tolerance value of 1×10^{-8}.

For each problem, while using the UTM, a numerical continuation strategy [29] is employed in which a very simple version of the problem is first solved. The solution to the simple problem is then used as a guess for the subsequent complex version of the problem. This process is continued until the original complex problem is solved that correspond to small values for all continuation parameters, i.e., ϵ values that are introduced in the previous section.

For brevity, this study excludes the analytical solutions, the dynamics for the costates, the Hamiltonian time-history plots, and the objective functional vs. the error parameter plots for examples 2-12. Shorthand notations of B- and S- are used for characterizing bang and singular parts of the control solution in the results. Recall that for each problem, PMP is used at each instant to select the best control from the available control options stated in the control law. All the

additional equations such as the Hamiltonian expression, the switching functions, the dynamics for the costates, the boundary equations for the costates and the Hamiltonian, and the control laws are generated in an automated manner using the UTM framework.

4.1 | Aly Chan Problem

Aly and Chan proposed a problem in Ref. [30] to demonstrate the utility of a method that they developed for solving singular control problems. This method is an extension of a modified quasi-linearization technique, which belongs to the category of indirect methods. The control solution for this problem is entirely singular, which can be obtained using the UTM as follows.

4.1.1 | Mathematical Problem Statement and Solution Process

The Aly problem is expressed as

$$\text{minimize } J = z_3(t_f) + \int_0^{t_f} \epsilon \cos u_{\text{TRIG}} \mathrm{d}t, \tag{17a}$$

$$\text{subject to } \dot{z}_1 = z_2, \tag{17b}$$

$$\dot{z}_2 = u, \tag{17c}$$

$$\dot{z}_3 = \frac{1}{2}(z_1^2 - z_2^2), \tag{17d}$$

$$\dot{t} = 1, \tag{17e}$$

where the UTM appends a small error, $\epsilon \cos u_{\text{TRIG}}$, into the functional, J, and converts the control, u, to $\sin u_{\text{TRIG}}$ such that $|u| \leq 1$ is satisfied. The equations of motion for the states are shown in Eqs. (17b)–(17e). The initial values for the states, $x_1(0)$ and $x_2(0)$, are 1 unit and 0 units, respectively. The Hamiltonian for this problem is given as

$$H = 0.5(z_1^2 + z_2^2) + \epsilon \cos u_{\text{TRIG}} + \lambda_{z_1} z_2 + \lambda_{z_2} \sin u_{\text{TRIG}} + \lambda_t, \tag{18}$$

which yields the switching function, H_1, as λ_{z_2}. The optimal control law generated using the UTM is

$$u^*_{\text{TRIG}} = \begin{cases} \arctan\left(\dfrac{H_1}{\epsilon}\right), \\ \arctan\left(\dfrac{H_1}{\epsilon}\right) + \pi, \end{cases} \tag{19}$$

which depends on the switching function, H_1. PMP is used to select the optimal control at each instance from among the two options listed in Eq. (19).

A numerical continuation approach with eight continuation sets is employed while using the UTM to solve this problem. In the first continuation set, the final value of the time is brought to $\pi/2$ s. Continuation sets 2-7 are used to lower the value of ϵ from 0.1 to 1×10^{-7}. The final continuation set is used to reduce the tolerance value for *bvp4c* from 1×10^{-4} to 1×10^{-6}.

4.1.2 | Results

The control solution obtained using the UTM is entirely singular and matches well with the analytical control solution as shown in the left subplot of Fig. 1. The switching function, shown in the right subplot of Fig. 1, stays at 0 value throughout, which further validates that the entire solution is singular. The results obtained using the PSM are full of jitters and not practical to implement in a real world scenario as shown in Fig. 1.

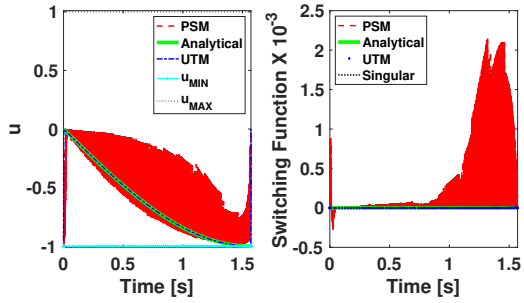

FIGURE 1 Control and switching function time-history plots for the Aly Chan problem.

Since H is not an explicit function of time, H is a constant. Additionally, using the final time condition [17], the final value of H is 0. Therefore, H has a constant value of 0 throughout, which is captured well by both the analytical method and the UTM as shown in the left subplot of Fig. 2. The PSM is unable to estimate the costates well and therefore yields a jittery Hamiltonian time-history solution.

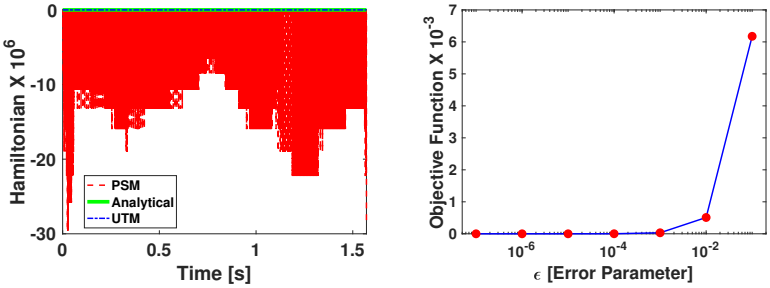

FIGURE 2 Hamiltonian time-history and cost history plots for the Aly Chan problem.

Decreasing ϵ beyond a certain low value does not improve the objective value as shown in the right subplot of Fig. 2. In this problem, $\epsilon < 1.0 \times 10^{-4}$ will result in very accurate solution. The optimal objective value obtained for this problem using the UTM is -5.9876$\times 10^{-6}$, which matches well with the literature. For the remaining problems in this paper, the values of ϵ are decreased only to an extent beyond which no further improvement in the objective value was found.

4.2 | Catalyst Mixing Problem

OCPs for tubular reactors can be solved for getting a catalyst distribution and temperature profile. The optimization of catalyst profile along the reactor would, in turn, control the final product yield in case of a multiple-steps reaction [6].

The catalyst mixing can be in any form, i.e., catalyst I at the beginning with catalyst II toward the end. The switching point and amount of catalyst coverage would depend on the reaction.

In the catalyst mixing problem [31], the reactions A<=>B->C take place in a tubular reactor at a constant temperature. The first reaction is reversible and is catalyzed by Catalyst I, while the second irreversible reaction is catalyzed by Catalyst II. The goal of this problem is to determine the optimal mixture of catalysts along the length t of the reactor to maximize the amount of product C. The production of final product C is limited by equilibrium of the reversible reaction.

4.2.1 | Mathematical Problem Statement and Solution Process

The catalyst mixing problem [31], while using the UTM, is expressed as

$$\text{minimize } J = -(1 - a_f - b_f) + \int_0^{t_f} \epsilon \cos u_{\text{TRIG}} \mathrm{d}t, \tag{20a}$$

$$\text{subject to } \dot{a} = -u(k_1 a - k_2 b), \tag{20b}$$

$$\dot{b} = u(k_1 a - k_2 b) - (1 - u)k_3 b, \tag{20c}$$

$$\dot{t} = 1, \tag{20d}$$

$$\text{where } u = \frac{1 + \sin u_{\text{TRIG}}}{2}. \tag{20e}$$

The dynamics for the states are shown in Eqs. (20b)–(20d). The UTM converts the control, u, to the form shown in Eq. (20e), such that $0 \leq u \leq 1$. The known boundary values for this problem are $a(0) = 1$, $b(0) = 0$, and $t_f = 4$ s. The constants used are $k_1 = 1$, $k_2 = 10$, and $k_3 = 1$.

The Hamiltonian and the switching function, H_1, for this problem are given as

$$H = \epsilon \cos u_{\text{TRIG}} - \lambda_a u(k_1 a - k_2 b) + \lambda_b(u(k_1 a - k_2 b) - (1 - u)k_3 b) + \lambda_t, \tag{21a}$$

$$H_1 = -\lambda_a(k_1 a - k_2 b) + \lambda_b((k_1 a - k_2 b) + k_3 b). \tag{21b}$$

The optimal control law, based on the switching function, H_1, is given as

$$u^*_{\text{TRIG}} = \begin{cases} \arctan\left(\dfrac{H_1}{2\epsilon}\right), \\ \arctan\left(\dfrac{H_1}{2\epsilon}\right) + \pi, \end{cases} \tag{22}$$

A numerical continuation strategy with seven continuation sets is employed while using the UTM to solve this problem. The final value of the time is brought to 4 s in the first continuation set. Continuation sets 2-6 are used to bring down the value of ϵ from 0.1 to 1×10^{-6}. In the final continuation set, the tolerance value for *bvp4c* is reduced from 1×10^{-4} to 1×10^{-6}.

4.2.2 | Results

A B-S-B type control solution is obtained using the UTM as shown in Fig. 3, which matches well with the literature [31]. The PSM yields a jittery solution for this problem. The switching function time history, shown in the right subplot of Fig. 3, is consistent with a B-S-B type control solution. The optimal objective value for this problem obtained using the

UTM is -0.19181.

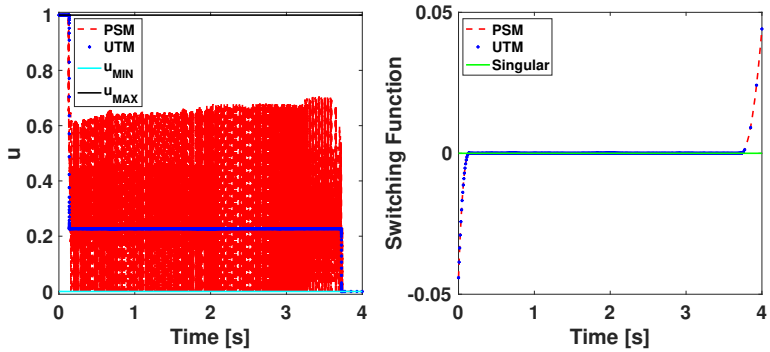

FIGURE 3 Control and switching function time-history plots for the catalyst mixing problem.

4.3 | Aly Problem

This is a linear-quadratic regulator problem presented by Aly [32] to demonstrate the utility of quasi-linearization technique for solving singular control problems. Aly and Chan developed an extension of the modified quasi-linearization method for the problem demonstrated in Ref. [30]; this problem is an extended version of the same. The objective of this problem is to minimize the integral of the sum of squares of the position and speed of a mobile unit over a fixed time interval.

4.3.1 | Mathematical Problem Statement and Solution Process

The Aly problem is described using the UTM as

$$\text{minimize } J = \int_0^{t_f} (0.5(x_1^2 + x_2^2) + \epsilon \cos u_{\text{TRIG}}) \mathrm{d}t, \tag{23a}$$

$$\text{subject to } \dot{x_1} = x_2, \tag{23b}$$

$$\dot{x_2} = u, \tag{23c}$$

$$\dot{t} = 1, \tag{23d}$$

where Eqs. (23b)–(23d) are the dynamics for the states. Similar to the Aly Chan problem, the UTM converts the control, u, to $\sin u_{\text{TRIG}}$ such that $|u| \leq 1$. The initial values for the states, $x_1(0)$ and $x_2(0)$, are 1 unit and 0 units, respectively. The value of t_f for this problem is 5 s. The Hamiltonian for this problem is given by

$$H = 0.5(x_1^2 + x_2^2) + \epsilon \cos u_{\text{TRIG}} + \lambda_{x_1} x_2 + \lambda_{x_2} \sin u_{\text{TRIG}} + \lambda_t. \tag{24}$$

The optimal control law obtained using the UTM and the switching function, H_1, for this problem are the same as that for the Aly Chan problem. Thus, the control law for this problem is given by Eq. (19). A numerical continuation strategy with five continuation sets is employed while using the UTM to solve this problem. The final value of time is

brought to 5 s in the first continuation set. The value of ϵ is brought down from 0.1 to 1×10^{-4} using continuation sets 2-4. The final continuation set reduces the tolerance value for *bvp4c* from 1×10^{-4} to 1×10^{-6}.

4.3.2 | Results

A B-S type control solution is obtained using the UTM as shown in Fig. 4, where the control stays at its lower bound and then switches to the singular arc. This is consistent with the results obtained in the literature for this problem. The PSM yields a solution with very few jitters for this problem. The switching function time history shown in the right subplot of Fig. 4 is consistent with a B-S type control solution. The optimal objective value for this problem obtained using the UTM is 0.37699.

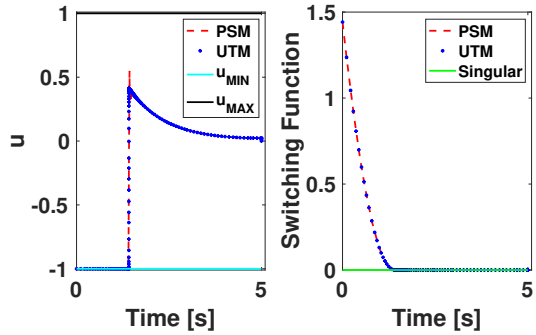

FIGURE 4 Control and switching function time-history plots for the Aly problem.

4.4 | Fishing Problem

Colin W. Clark described a fishing problem in *Mathematical Bioeconomics* chapter of Ref. [33]. For this fishing problem, the objective is to maximize the net revenue of fishing over a fixed time interval. This problem is mathematically described as follows.

4.4.1 | Mathematical Problem Statement and Solution Process

The fishing problem is expressed as

$$\text{minimize } J = \int_0^{t_f} \left(-\left[E - \frac{c}{x}\right] uU_{\text{MAX}} + \epsilon \cos u_{\text{TRIG}}\right) \mathrm{d}t, \tag{25a}$$

$$\text{subject to } \dot{x} = rx\left(1 - \frac{x}{k}\right) - uU_{\text{MAX}}, \tag{25b}$$

$$\dot{t} = 1, \tag{25c}$$

where the coefficient, $E - c/x$, accounts the greater fishing cost for a low fish population [34]. The dynamics for the states are shown in Eq. (25b) and Eq. (25c), where x is the fish population and u is the fishing activity. The UTM converts the control u to $0.5(1 + \sin u_{\text{TRIG}})$ such that $0 \leq u \leq 1$. The known boundary values for this problem are $x(0) = 70$ and t_f

= 10 s. The constants used are $E = 1$, $c = 17.5$, $r = 0.71$, $k = 80.5$, and $U_{MAX} = 20$.

The Hamiltonian and the switching function (H_1) for this problem are

$$H = -\left(E - \frac{c}{x}\right) u U_{MAX} + \epsilon \cos u_{TRIG} + \lambda_x \left(rx\left[1 - \frac{x}{k}\right] - u U_{MAX}\right) + \lambda_t, \tag{26a}$$

$$H_1 = U_{MAX}\left(\frac{c}{x} - E - \lambda_x\right). \tag{26b}$$

The optimal control law for this problem has the same form as Eq. (16) from the catalyst mixing problem with H_1 given by Eq. (16). The numerical continuation approach with six continuation sets is used to solve this problem. The first continuation set solves for the final time as 10 s. Continuation sets 2-4 bring down the value of ϵ from 0.1 to 1×10^{-5}. In the final continuation set, *bvp4c*'s tolerance value is reduced from 1×10^{-4} to 1×10^{-6}.

4.4.2 | Results

A B-S-B type control solution is obtained using the UTM and is shown in Fig. 5, which is in excellent agreement with the solution reported in the literature [33]. The PSM yields a jittery solution for this problem as well. The switching function time history shown in the right subplot of Fig. 5 further validates a B-S-B type control solution. The optimal objective value for this problem found using the UTM is -106.906.

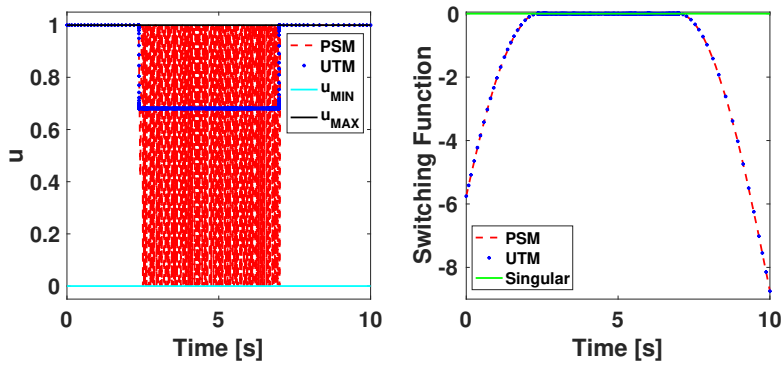

FIGURE 5 Control and switching function time-history plots for the fishing problem.

4.5 | Bryson Problem

Bryson and Ho [26] described an autonomous linear system of second order with one control variable and a quadratic performance index in state variables only, popularly known as the Bryson problem. The mathematical problem statement, solution process using the UTM, and the corresponding results obtained are discussed as follows.

4.5.1 | Mathematical Problem Statement and Solution Process

Bryson problem is written as

$$\text{minimize } J = \int_0^{t_f} (0.5z_1^2 + \epsilon \cos u_{\text{TRIG}})\mathrm{d}t, \tag{27a}$$

$$\text{subject to } \dot{z_1} = u + z_2, \tag{27b}$$

$$\dot{z_2} = -u, \tag{27c}$$

$$\dot{t} = 1, \tag{27d}$$

where Eqs. (27b)–(27d) describe the dynamics for the states. The UTM converts the control u to $\sin u_{\text{TRIG}}$ such that $|u| \leq 1$. The known boundary values for this problem are $z_1(0) = 0.5$, $z_2(0) = z_1(t_f) = z_2(t_f) = 0$, and $t_f = 1.5$ s. The Hamiltonian for this problem is given by

$$H = 0.5z_1^2 + \epsilon \cos u_{\text{TRIG}} + \lambda_{z_1}(u + z_2) - \lambda_{z_2} u + \lambda_t. \tag{28}$$

The optimal control law is based on the switching function, $H_1 = \lambda_{z_1} - \lambda_{z_2}$, and has the same form as the Aly Chan and Aly problems. Thus, Eq. (19) can be used as the optimal control law for this problem. A numerical continuation strategy with seven continuation sets is employed while using the UTM to solve this problem. The final values of the two states and time are brought to values of 0, 0, and 1.5 s, respectively, in the first continuation set. Continuation sets 2-4 are used to bring down the value of ϵ from 0.1 to 1×10^{-4}.

4.5.2 | Results

The control solution obtained using the UTM for this problem is of B-S-B type as shown in Fig. 6, which is in excellent agreement with the literature [26]. The PSM yields a slight jittery solution for this problem. The switching function time history shown in the right subplot of Fig. 6 is consistent with a B-S-B type control solution. The optimal objective value for this problem obtained using the UTM is 0.29945.

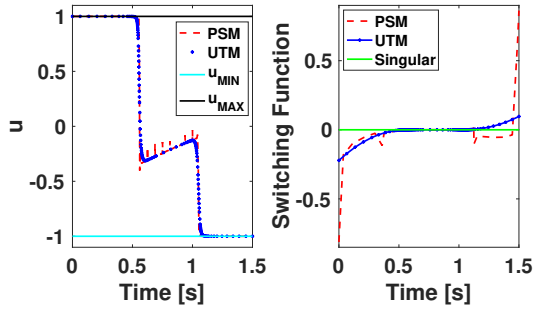

FIGURE 6 Control and switching function time-history plots for the Bryson problem.

4.6 | Luus Problem

In Ref. [35], Luus described a singular control problem that has an easy analytical solution, but also has a difficult numerical solution while employing iterative dynamic programming. The mathematical problem statement, solution process using the UTM, and the results for this problem are discussed as follows.

4.6.1 | Mathematical Problem Statement and Solution Process

Luus problem is expressed as

$$\text{minimize } J = \int_0^{t_f} (0.5z^2 + \epsilon \cos u_{\text{TRIG}}) \mathrm{d}t, \tag{29a}$$

$$\text{subject to } \dot{z} = u, \tag{29b}$$

$$\dot{t} = 1, \tag{29c}$$

where dynamics for the states are shown in Eq. (29b) and Eq. (29c). The UTM converts the control u to $\sin u_{\text{TRIG}}$ such that $|u| \leq 1$. The initial value of the state, $z(0)$, is 1 unit and the final value of time, t_f, is 2 s. The Hamiltonian for this problem is

$$H = 0.5z^2 + \epsilon \cos u_{\text{TRIG}} + \lambda_z \sin u_{\text{TRIG}} + \lambda_t. \tag{30}$$

The optimal control law for this problem has the same form as Aly Chan and Aly problems, which is given by Eq. (19). For this problem, the switching function, H_1 is λ_z. A numerical continuation strategy comprising 10 continuation sets is used to solve this problem. In the first continuation set, the final time is brought to 2 s. Continuation sets 2-10 are used to bring down the value of ϵ from 0.1 to 1×10^{-10}.

4.6.2 | Results

A B-S type control solution is obtained using the UTM and is shown in Fig. 3, which matches well with the literature [35]. The PSM yields a slight jittery solution for the singular control phase of this problem. The switching function time history shown in the right subplot of Fig. 3 is consistent with a B-S-B type control solution. The optimal objective value for this problem obtained using the UTM is 0.1667.

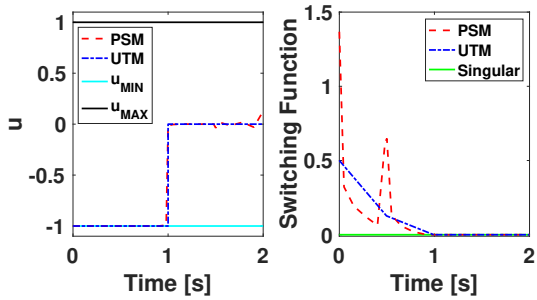

FIGURE 7 Control and switching function time-history plots for the Luus problem.

4.7 | Jennings Problem

Jennings et al. described a minimum-time problem in Ref. [36] to demonstrate an optimal control software called MISER3. The mathematical problem statement, solution strategy using the UTM, and the results obtained for this problem are discussed as follows.

4.7.1 | Mathematical Problem Statement and Solution Process

Jennings problem is described as

$$\text{minimize } J = t_f + \int_0^{t_f} \epsilon \cos u_{\text{TRIG}} \, dt, \tag{31a}$$

$$\text{subject to } \dot{z}_1 = u, \tag{31b}$$

$$\dot{z}_2 = \cos z_1, \tag{31c}$$

$$\dot{z}_3 = \sin z_1, \tag{31d}$$

$$u = 2 \sin u_{\text{TRIG}}, \tag{31e}$$

where Eqs. (31b)–(31d) represent the dynamics for the states. The UTM converts the control u to $2 \sin u_{\text{TRIG}}$ such that $|u| \leq 2$. The known boundary values for this problem include $z_1(0) = \pi/2$, $z_2(0) = 4$, and $z_3(0) = z_2(t_f) = z_3(t_f) = 0$. The Hamiltonian can then be written as

$$H = \epsilon \cos u_{\text{TRIG}} + \lambda_{z_1} u + \lambda_{z_2} \cos z_1 + \lambda_{z_3} \sin z_1 + \lambda_t. \tag{32}$$

The optimal control law obtained using the UTM is

$$u^*_{\text{TRIG}} = \begin{cases} \arctan\left(\dfrac{2H_1}{\epsilon}\right), \\ \arctan\left(\dfrac{2H_1}{\epsilon}\right) + \pi, \end{cases} \tag{33}$$

where the switching function, $H_1 = \lambda_{z_1}$. A numerical continuation strategy with three continuation sets is used to solve this problem. The final values of z_2 and z_3 are brought to 0 in the first continuation set. Continuation sets 2-3 bring down the value of ϵ from 0.1 to 1×10^{-3}.

4.7.2 | Results

A B-S type control solution is obtained using the UTM as shown in Fig. 8, where the control stays at its upper bound and then switches to the singular arc. The result obtained using the UTM matches very well with the results obtained in the literature [36]. The PSM yields a solution with very few jitters for this problem around the switching junction. The switching function time history shown in the right subplot of Fig. 8 is consistent with a B-S type control solution. The optimal objective value for this problem obtained using the UTM is 4.3212 s.

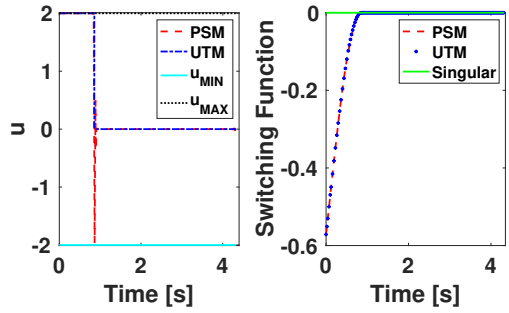

FIGURE 8 Control and switching function time-history plots for the Jennings problem.

4.8 | Bressan Problem

This problem is included in Ref. [37] for demonstration of the complicated traditional indirect methodology to obtain the singular control law. The mathematical problem statement, UTM based solution approach, and the results obtained for this problem are discussed as follows.

4.8.1 | Mathematical Problem Statement and Solution Process

The Bressan problem is described as

$$\text{minimize } J = -z_{3_f} + \int_0^{t_f} \epsilon \cos u_{\text{TRIG}} \mathrm{d}t, \tag{34a}$$

$$\text{subject to } \dot{z_1} = u, \tag{34b}$$

$$\dot{z_2} = -z_1, \tag{34c}$$

$$\dot{z_3} = z_2 - z_1^2, \tag{34d}$$

$$\dot{t} = 1, \tag{34e}$$

where the dynamics for the states are shown in Eqs. (34b)–(34e). The UTM converts the control, u, to $\sin u_{\text{TRIG}}$ such that $|u| \leq 1$. The known boundary values for this problem are $z_1(0) = z_2(0) = z_3(0) = 0$, and $t_f = 10$ s. The Hamiltonian for this problem is

$$H = \epsilon \cos u_{\text{TRIG}} + \lambda_{z_1} u - \lambda_{z_2} z_1 + \lambda_{z_3}(z_2 - z_1^2) + \lambda_t. \tag{35}$$

The optimal control law for this problem has the same form as the control law for the Aly Chan problem, which is given by Eq. (19). The switching function used in this problem is $H_1 = \lambda_{z_1}$.

A numerical continuation approach with five continuation sets is employed while using the UTM to solve this problem. In the first continuation set, the final value of the time is brought to 10 s. Continuation sets 2-4 are used to bring down the value of ϵ from 0.1 to 1×10^{-4}. The final continuation set reduces error tolerance of *bvp4c* from 1×10^{-4} to 1×10^{-6}.

4.8.2 | Results

A B-S type control solution is obtained using the UTM as shown in Fig. 9, where the control stays at its lower bound and then switches to the singular arc. This is consistent with the results obtained in the literature [37]. The PSM yields few jitters in the singular part of the solution. In the right subplot of Fig. 9, the switching function time history is shown, which is consistent with a B-S type control solution. The optimal objective value for this problem obtained using the UTM is -55.5556.

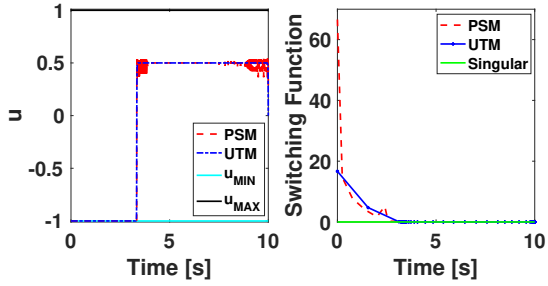

FIGURE 9 Control and switching function time-history plots for the Bressan problem.

4.9 | Two-Stage Continuous Stirred-Tank Reactor Problem

In a continuous stirred tank reactor (CSTR), the temperature is controlled using jacketed cooling. It is a tricky task to find an optimal control signal for a CSTR. The temperature in the tank influences the reaction rate and kinetics (and vice versa), while the temperature in the cooling jacket acts a control signal [38].

4.9.1 | Mathematical Problem Statement and Solution Process

A two stage CSTR system is considered here [39, 40]. A first order reversible reaction is carried out in a two-stage, four-state-variable system. The reaction initiates from a state of equilibrium and reaches a state with maximum rate with respect to the temperature. This problem is described as

$$\text{minimize } J = x_1(t_f)^2 + x_2(t_f)^2 + x_3(t_f)^2 + x_4(t_f)^2 + \int_0^{t_f} (\epsilon_1 \cos u_{1_{\text{TRIG}}} + \epsilon_2 \cos u_{2_{\text{TRIG}}})\text{dt}, \tag{36a}$$

$$\text{subject to } \dot{x}_1 = -3x_1 + g_1, \tag{36b}$$

$$\dot{x}_2 = -11.1558x_2 + g_1 - 8.1558(x_2 + 0.1592)u_1, \tag{36c}$$

$$\dot{x}_3 = 1.5(0.5x_1 - x_3) + g_2, \tag{36d}$$

$$\dot{x}_4 = 0.75x_2 - 4.9385x_4 + g_2 - 3.4385(x_4 + 0.122)u_2, \tag{36e}$$

$$\dot{t} = 1, \tag{36f}$$

$$\text{where } g_1 = 1.5X10^7(0.5251 - x_1)e^{\frac{-10}{x_2+0.6932}} - 1.5X10^{10}(0.4748 + x_1)e^{\frac{-15}{x_2+0.6932}} - 1.428,$$
$$g_2 = 1.5X10^7(0.4236 - x_2)e^{\frac{-10}{x_4+0.656}} - 1.5X10^{10}(0.5764 + x_3)e^{\frac{-15}{x_4+0.656}} - 0.5086,$$
$$u_1 = \sin u_{1_{\text{TRIG}}}, u_2 = \sin u_{2_{\text{TRIG}}}.$$

The dynamics for the states are shown in Eqs. (36b)–(36f). The known boundary values for this problem are given as $x_1(0)$ = 0.1962, $x_2(0)$ = -0.0372, $x_3(0)$ = 0.0946,$x_4(0)$ = 0, and t_f = 0.32353 s.

The form of the optimal control law for both the controls in this problem, u_1 and u_2, is the same as that for the Aly Chan problem. Thus, Eq. (19) is used for both the controls, with switching function values, H_{1_1} and H_{1_2} as

$$H_{1_1} = -8.1558\lambda_{x_2}(x_2 + 0.1592), \tag{38a}$$
$$H_{1_2} = -3.4385\lambda_{x_4}(x_4 + 0.122). \tag{38b}$$

A numerical continuation with seven continuation sets is used to solve this problem. Continuation sets 1-7 are used to bring down the value of ϵ_1 and ϵ_2 from 1 to 1×10^{-6}. The final continuation set is used to reduce the tolerance value for *bvp4c* from 1×10^{-4} to 1×10^{-6}.

4.9.2 | Results

A B-S-B type control solution is obtained for u_1 using the UTM and is shown in the left subplot of Fig. 3. The u_1 solution obtained using the UTM is of higher resolution than the corresponding solutions obtained using the PSM and Ref. [39]. A B-B type solution is obtained using the UTM for u_2, as shown in the right subplot of Fig. 3, which is in excellent agreement with the solutions obtained using the PSM and Ref. [39] (indicated as Luus in the legend of the plot). The optimal objective value for this problem obtained using the UTM is 1.2985×10^{-8}.

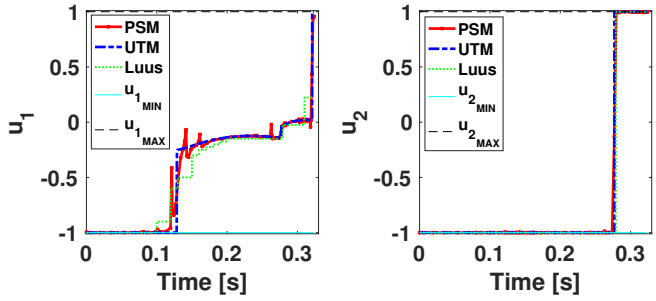

FIGURE 10 Controls time-history plots for the CSTR problem.

4.10 | Distillation Problem

Static and dynamic characteristic behaviour of high-purity distillation columns is challenging to control. The behavior of such columns is intrinsically non-linear. Thus, since linear control methods often become inadequate, non-linear control strategies or logarithmic variable transformations are used [41]. A distillation problem from the literature [11] is discussed as follows.

4.10.1 | Mathematical Problem Statement and Solution Process

A distillation column with 30 trays for separation of a binary mixture is considered in this problem with 32 states [11]. The operating region for this problem was chosen to be ± 10 % around the steady state values. This problem is mathematically described as

$$\text{minimize } J = \int_0^{t_f} (x_1 - 0.995)^2 + \epsilon \cos u_{\text{TRIG}} \text{dt}, \tag{39a}$$

$$\text{subject to } \dot{x}_1 = \frac{1}{M_{\text{COND}}} V(y_2 - x_1), \tag{39b}$$

$$\dot{x}_j = \frac{1}{M_{\text{TRAY}}} (L(x_{j-1} - x_j) - V(y_j - x_{j+1})) \quad j = 2, \cdots, 16, \tag{39c}$$

$$\dot{x}_{17} = \frac{1}{M_{\text{TRAY}}} (F\, x_{\text{FEED}} + L x_{16} - (F + L) x_{17} - V(y_{17} - x_{18})), \tag{39d}$$

$$\dot{x}_k = \frac{1}{M_{\text{TRAY}}} ((F + L)(x_{j-1} - x_j) - V(y_j - x_{j+1})) \quad k = 18..31, \tag{39e}$$

$$\dot{x}_{32} = \frac{1}{M_{\text{REB}}} ((F + L) x_{31} - (F - D) x_{32} - V y_{32}), \tag{39f}$$

$$\dot{t} = 1, \tag{39g}$$

$$\text{where } \gamma_{A_i} = exp\left(-log(x_i + L_{12}(1 - x_i)) + \frac{L_{12}(1 - x_i)}{x_i + L_{12}(1 - x_i)} - \frac{L_{21}}{L_{21} x_i + (1 - x_i)}\right),$$

$$\gamma_{B_i} = exp\left(-log((1 - x_i) + L_{21} x_i) + \frac{L_{21} x_i}{L_{21} x_i + (1 - x_i)} - \frac{L_{12}}{x_i + L_{12}(1 - x_i)}\right),$$

$$vol_i = \frac{\gamma_{A_i}}{\gamma_{B_i}}, y = \frac{1.7 x_i vol_i}{1 + (vol_i - 1) x_i}, \forall i \in [1, 32], L = Du, V = L + D.$$

In the above equations, V and L are vapor and liquid flow rates, respectively; x and y are liquid and vapor mole fractions, respectively; the molar holdup for tray i, M_{TRAY}, is 0.25; the molar holdup for condenser, M_{COND}, is 0.5; the molar holdup for reboiler, M_{REB}, is 1; the distillate flowrate, D, is 0.2; the feed flow rate, F, is 0.4; the constant relative volatility is 1.6. The feed stream is introduced at the middle of the column on stage 17 and has a composition of x_F = 0.5. Wilson activity coefficient model parameters, L_{12} and L_{21} are 1.618147731 and 0.50253532, respectively.

The UTM converts the control u to 4 sin u_{TRIG} + 6 such that $2 \leq u \leq 10$. The control law obtained using the UTM is

$$u^*_{\text{TRIG}} = \begin{cases} \arctan\left(\dfrac{4H_1}{\epsilon}\right), \\ \arctan\left(\dfrac{4H_1}{\epsilon}\right) + \pi, \end{cases} \tag{40}$$

The switching function used in the control law is very long and has been excluded from this paper for brevity.

The known boundary values are $x_1(0) = 0.97339252747326$, $x_2(0) = 0.95790444111368$, $x_3(0) = 0.93963386412300$, $x_4(0) = 0.91821664141445$, $x_5(0) = 0.89334470835687$, $x_6(0) = 0.86483847458375$, $x_7(0) = 0.83273815158540$, $x_8(0) = 0.79739606050503$, $x_9(0) = 0.75953677930557$, $x_{10}(0) = 0.72024599485005$, $x_{11}(0) = 0.68086442052299$, $x_{12}(0) = 0.64280066114073$, $x_{13}(0) = 0.60731690633284$, $x_{14}(0) = 0.57535610831821$, $x_{15}(0) = 0.54745802413982$, $x_{16}(0) = 0.52377039366803$, $x_{17}(0) = 0.50412746272762$, $x_{18}(0) = 0.49037636253375$, $x_{19}(0) = 0.47205010235430$, $x_{20}(0) = 0.44820197086528$, $x_{21}(0) = 0.41811322760501$, $x_{22}(0) = 0.38159643880344$, $x_{23}(0) = 0.33930475369667$, $x_{24}(0) = 0.29288862241213$, $x_{25}(0) = 0.24483954092739$, $x_{26}(0) = 0.19799745874320$, $x_{27}(0) = 0.15490859777720$, $x_{28}(0) = 0.11732282321971$, $x_{29}(0) = 0.08601628593205$, $x_{30}(0) = 0.06092130595344$, $x_{31}(0) = 0.04141387478979$, $x_{32}(0) = 0.02660747253544$, and $t_f = 240$ s.

A numerical continuation approach with 10 continuation sets is employed while using the UTM to solve this problem. In the first continuation set, the final time is brought to 240 s. Continuation sets 2-10 are used to bring down the value of ϵ from 0.1 to 2×10^{-10}.

4.10.2 | Results

The control solution obtained using the UTM matches well with the results reported in Ref. [16], both of which are shown in Fig. 11. The initial part of u is an upper bang followed by a singular arc. Despite numerous efforts, no results could be generated using the PSM for this problem.

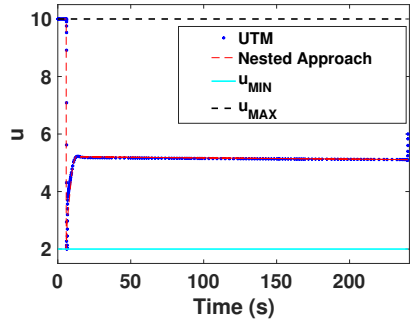

FIGURE 11 Comparison of the control time history plot for the distillation problem with 32 states between the UTM and the Nested Approach [16].

4.11 | Williams-Otto Problem

This problem deals with a Williams-Otto semi-batch reactor introduced by Forbes and comprises two bounded controls and a scalar state constraint [7]. Three irreversible reactions take place in a reactor in which one reactant is already present and the second reactant is continuously fed. The bounded controls for this problem are inlet flow rate of the continuously fed reactant and the scaled cooling water temperature. The state constraint is upon the reactor temperature. The objective is to maximize the conversion to the desired products.

4.11.1 | Mathematical Problem Statement and Solution Process

The Williams-Otto problem is mathematically described using the UTM as

$$\text{minimize } J = x_9(t_f) + \int_0^{t_f} \left[\epsilon_1 \cos u_{1_{\text{TRIG}}} + \epsilon_2 \cos u_{2_{\text{TRIG}}} + \epsilon_3 \sec\left(\frac{\pi}{2}\left(\frac{2x_7 - x_{7_{\text{MAX}}} - x_{7_{\text{MIN}}}}{x_{7_{\text{MAX}}} - x_{7_{\text{MIN}}}}\right)\right)\right] \text{dt}, \tag{41a}$$

$$\text{subject to } \dot{x}_1 = -\frac{x_1 u_2}{1000 x_8} - k_1 \eta_1 x_1 x_2, \tag{41b}$$

$$\dot{x}_2 = \frac{u_2(1 - x_2)}{1000 x_8} - k_1 \eta_1 x_1 x_2 - k_2 \eta_2 x_2 x_3, \tag{41c}$$

$$\dot{x}_3 = -\frac{x_3 u_2}{1000 x_8} + k_7 \eta_1 x_1 x_2 - k_3 \eta_2 x_2 x_3 - k_6 \eta_3 x_3 x_4, \tag{41d}$$

$$\dot{x}_4 = -\frac{x_4 u_2}{1000 x_8} + k_2 \eta_2 x_2 x_3 - k_4 \eta_3 x_3 x_4, \tag{41e}$$

$$\dot{x}_5 = -\frac{x_5 u_2}{1000 x_8} + k_3 \eta_2 x_2 x_3, \tag{41f}$$

$$\dot{x}_6 = -\frac{x_6 u_2}{1000 x_8} + k_5 \eta_3 x_3 x_4, \tag{41g}$$

$$\dot{x}_7 = \frac{u_2(T_{\text{IN}} - x_7)}{1000 x_8} + k_8 \eta_1 x_1 x_2 + k_9 \eta_2 x_2 x_3 + k_{10} \eta_3 x_3 x_4 - l_1 x_7 + l_2 u_1, \tag{41h}$$

$$\dot{x}_8 = \frac{u_2}{1000}, \tag{41i}$$

$$\dot{x}_9 = -5554.1(k_2 \eta_2 x_2 x_3 - k_4 \eta_3 x_3 x_4) x_8 - k_{11} \eta_2 x_2 x_3 x_8, \tag{41j}$$

$$\dot{t} = 1, \tag{41k}$$

$$\text{where } \eta_1 = e^{\left(\frac{-1000 b_2}{x_7 + 273.15}\right)}, \eta_2 = e^{\left(\frac{-8333.3}{x_7 + 273.15}\right)}, \eta_3 = e^{\left(\frac{-11111}{x_7 + 273.15}\right)}, u_1 = 0.04 \sin u_{2_{\text{TRIG}}} + 0.06, u_2 = 2.892(1 + \sin u_{1_{\text{TRIG}}}).$$

The UTM is thus able to impose the control constraints: $0.02 \leq u_1 \leq 0.1$ and $0 \leq u_2 \leq 5.784$, and the path constraint: $60 \leq x_7 \leq 90$ with $x_{7_{\text{MIN}}}$ and $x_{7_{\text{MAX}}}$ as 60 and 90, respectively. The optimal control law obtained using the UTM is

$$u^*_{1_{\text{TRIG}}} = \begin{cases} \arctan\left(\dfrac{0.04 H_{1_1}}{\epsilon}\right), \\ \arctan\left(\dfrac{0.04 H_{1_1}}{\epsilon}\right) + \pi, \end{cases} \tag{42a}$$

$$u^*_{2_{\text{TRIG}}} = \begin{cases} \arctan\left(\dfrac{2.892 H_{1_2}}{\epsilon}\right), \\ \arctan\left(\dfrac{2.892 H_{1_2}}{\epsilon}\right) + \pi, \end{cases} \tag{42b}$$

where

$$H_{1_1} = 0.04 l_2 \lambda_{x_7}, \quad H_{1_2} = \frac{2.892(-\lambda_{x_1} x_1 + \lambda_{x_2}(1 - x_2) - \lambda_{x_3} x_3 - \lambda_{x_4} x_4 - \lambda_{x_5} x_5 - \lambda_{x_6} x_6 + \lambda_{x_7}(T_{\text{IN}} - x_6) + \lambda_{x_8} x_8)}{1000 x_8}. \tag{43a}$$

To implement the state path constraint on x_7, the objective functional, J, is modified by adding a secant term inside the integral. The modified J leads to a modified Hamiltonian, which ultimately leads to a modification in the dynamics for λ_{x_7} while using Eq. (4). The new modified and complicated dynamics for λ_{x_7} is excluded from this study for brevity.

The known boundary values for this problem are $x_1(0) = 1$, $x_2(0) = x_3(0) = x_4(0) = x_5(0) = x_6(0) = x_9(0) = 0$, $x_7(0) = 65$, $x_8(0) = 2$, and $t_f = 1000$ s. The constants used in this problem are $k_1 = 1659900$, $k_2 = 721170000$, $k_3 = 1442340000$, $k_4 = 1337250000000$, $k_5 = 4011750000000$, $k_6 = 2674500000000$, $k_7 = 3319800$, $k_8 = 104656218.9$, $k_9 = 27285184270$,

k_{10} = 144655676400000, k_{11} = 181605029400, I_1 = 0.0002434546857, I_2 = 0.24345468574, T_{IN} = 35, and b_2 = 6.6667.

A numerical continuation technique with 14 continuation sets is adopted while using the UTM to solve this problem. In the first continuation set, the final values of the time and x_8 are brought to 1000 s and 5, respectively. Continuation sets 2-7 are used to bring down the values of ϵ_1 and ϵ_2 (corresponding to the constraints on u_1 and u_2, respectively) from 0.1 to 2×10^{-7}. Similarly, continuation sets 8-13 are used to bring down the values of ϵ_3 (corresponding to the constraint on x_7) from 0.1 to 1×10^{-6}.

4.11.2 | Results

A B-B-S-B-B-B type control solution is obtained for u_1 using the UTM and is shown in the left subplot of Fig. 12. The u_1 solution obtained using the UTM matches well with the corresponding solutions obtained using the PSM without the spikes that exist in the PSM solution. A B-B type solution is obtained using the UTM for u_2 as shown in the right subplot of Fig. 12, which is in excellent agreement with the solutions obtained using the PSM.

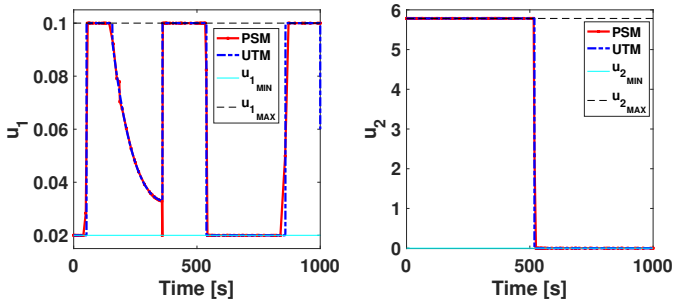

FIGURE 12 Controls time-history plots for the Williams-Otto problem.

Fig. 13 depicts the time history for x_7, which clearly shows that the lower bound on x_7 is active. The UTM is able to capture the lower constraint on x_7 while simultaneously solving for the singular control. These solutions showcase the ability of the UTM to handle several control and state constraints simultaneously, which has been traditionally a daunting task while using indirect methods. The optimal objective value for this problem obtained using the UTM is -4768.271, which is very close to the solutions obtained in the literature.

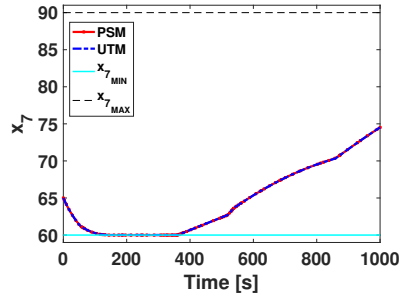

FIGURE 13 x_7 time-history plots for the Williams-Otto problem.

4.12 | Summary of Results

All computations for the UTM were performed on a personal computer with a 2.6 GHz Intel® Core™ i7 processor and 16 GB RAM using MATLAB 2019a built-in BVP solver, *bvp4c*. The objective values and computation times obtained for the 11 problems solved in this study using the nested and simultaneous approaches, a PSM (GPOPS-II), and the UTM are summarized in Table 2. Note that in Table 2, ϵ_c and ϵ_s are error parameters corresponding to control and state constraints, respectively.

The nested approach, the simultaneous approach, and the PSM are direct methods whereas the UTM is an indirect method. Although the computation times required for the simultaneous approach is very small compared to the UTM, vectorization and customizing the code while using MATLAB's *bvp4c* would result in much lesser computation times while employing the UTM. Future work includes implementing vectorization of the UTM code and creating a custom *bvp4c* code that would take substantially lesser time than indicated in this study.

TABLE 2 Results summary.

Problem	Nested Approach		Simultaneous Approach		PSM		UTM			
	Objective	Time (s)	Objective	Time (s)	Objective	Time (s)	Objective	Time (s)	ϵ_c	ϵ_s
Aly-Chan [30]	0	60.30	0	0.78	3.3180×10^{-7}	3.77	-5.9876×10^{-6}	10.50	1×10^{-7}	-
Catalyst Mixing [31]	-0.19181	22.50	-0.19181	0.90	-0.19181	20.04	-0.19181	19.23	1×10^{-6}	-
Aly [32]	0.37699	132.03	0.37699	0.33	0.37699	0.29	0.37699	3.53	1×10^{-7}	-
Fishing [34]	-106.9060	123.20	-106.9060	0.49	-106.9067	31.43	-106.9060	6.00	1×10^{-4}	-
Bryson [26]	0.29945	32.30	0.29945	0.48	0.29945	3.20	0.29945	12.04	1×10^{-4}	-
Luus [35]	0.1667	23.10	0.1667	0.17	0.1667	0.43	0.1667	12.21	1×10^{-10}	-
Jennings [36, 42]	4.3212	17.50	4.3212	0.22	4.3212	0.48	4.3212	6.659	1×10^{-3}	-
Bressan [37]	-55.5556	24.80	-55.5556	0.33	-55.5556	5.88	-55.5556	5.62	1×10^{-4}	-
Two-Stage CSTR [39, 40]	-	-	2.3350×10^{-9}	2.05	1.38512×10^{-9}	4.80	1.2985×10^{-8}	28.10	1×10^{-6}	-
Distillation [11]	6.4538×10^{-4}	1579.1	6.4540×10^{-4}	84.21	-	-	6.4386×10^{-4}	319.40	2×10^{-10}	-
Williams-Otto [7]	-	-	-4768.314	34.45	-4768.313	7.18	-4768.271	165.13	2×10^{-7}	1×10^{-6}

5 | CONCLUSIONS

In this study, eight classical singular control problems with known analytical solutions and three complex problems from the chemical engineering domain comprising singular controls were solved using the Uniform Trigonometrization Method (UTM). The UTM generates analytical singular control laws and offers an alternative to the existing direct methods in the literature that are devised to numerically solve for the singular control. The results obtained using the UTM in this study were found to be in excellent match with the results obtained in the literature. Furthermore, the results obtained using the UTM were found to be of higher resolution than the jittery solutions obtained using a pseudo-spectral method (PSM) based solver for many problems in this study. Unlike certain other methods in the literature that are only devised to solve singular control problems, the UTM is able to handle bang-bang and singular controls along with state path constraints in a simultaneous manner. This utility of the UTM is demonstrated through the Williams-Otto problem in this study. The UTM is shown capable of solving problems that consist of control inputs with their distinct bang-bang or singular arcs.

REFERENCES

[1] Rangaiah GP, Bonilla-Petriciolet A. Multi-objective optimization in chemical engineering: developments and applications. John Wiley & Sons; 2013.

[2] Dutta S. In: Formulation of Optimization Problems in Chemical and Biochemical Engineering Cambridge University Press; 2016. p. 12–39.

[3] Srinivasan B, Palanki S, Bonvin D. Dynamic optimization of batch processes: I. Characterization of the nominal solution. Computers & Chemical Engineering 2003;27(1):1–26.

[4] Shin HS, Lim HC. Optimization of metabolite production in fed-batch cultures: use of sufficiency and characteristics of singular arc and properties of adjoint vector in numerical computation. Industrial & engineering chemistry research 2007;46(8):2526–2534.

[5] Nie Y, Witt PM, Agarwal A, Biegler LT. Optimal active catalyst and inert distribution in catalytic packed bed reactors: ortho-xylene oxidation. Industrial & Engineering Chemistry Research 2013;52(44):15311–15320.

[6] Jaczson R. Optimal use of mixed catalysts for two successive chemical reactions. Journal of Optimization Theory and Applications 1968;2(1):27–39.

[7] Hannemann-Tamás R, Marquardt W. How to verify optimal controls computed by direct shooting methods?–A tutorial. Journal of Process Control 2012;22(2):494–507.

[8] Ko DY, Stevens WF. Studies of singular solutions in dynamic optimization: II. Optimal singular design of a plug-flow tubular reactor. AIChE Journal 1971;17(1):160–166.

[9] Smets IY, Dochain D, Van Impe JF. Optimal temperature control of a steady-state exothermic plug-flow reactor. AIChE Journal 2002;48(2):279–286.

[10] Hicks J, Mohan A, Ray WH. The optimal control of polymerisation reactors. The Canadian Journal of Chemical Engineering 1969;47(6):590–597.

[11] Hahn J, Edgar TF. An improved method for nonlinear model reduction using balancing of empirical gramians. Computers & chemical engineering 2002;26(10):1379–1397.

[12] Luus R. Optimal control of batch reactors by iterative dynamic programming. Journal of Process Control 1994;4(4):218–226.

[13] MacGregor J. Control of polymerization reactors. In: Dynamics and Control of Chemical Reactors and Distillation Columns Elsevier; 1988.p. 31–35.

[14] Ogunye A, Ray W. Optimal control policies for tubular reactors experiencing catalyst decay: II. Multiple-bed semiregenerative reactors. AIChE Journal 1971;17(2):365–371.

[15] Von Stryk O, Bulirsch R. Direct and indirect methods for trajectory optimization. Annals of operations research 1992;37(1):357–373.

[16] Chen W, Biegler LT. Nested direct transcription optimization for singular optimal control problems. AIChE Journal 2016;62(10):3611–3627.

[17] Longuski JM, Guzmán JJ, Prussing JE. Optimal control with aerospace applications. Springer; 2014.

[18] Chen W, Ren Y, Zhang G, Biegler LT. A simultaneous approach for singular optimal control based on partial moving grid. AIChE Journal 2019;65(6):e16584.

[19] Silva C, Trélat E. Smooth regularization of bang-bang optimal control problems. IEEE Transactions on Automatic Control 2010;55(11):2488–2499.

[20] Mall K, Grant MJ. Epsilon-Trig Regularization Method for Bang-Bang Optimal Control Problems. Journal of Optimization Theory and Applications 2017;174(2):500–517.

[21] Mall K. Advancing Optimal Control Theory for Solving Complex Aerospace Problems. PhD thesis, Purdue University; 2018.

[22] Mall K, Taheri E. Unified Trigonometrization Method for Solving Optimal Control Problems in Atmospheric Flight Mechanics. In: AIAA Scitech 2020 Forum; 2020. p. 0022.

[23] Mall K, Grant MJ, Taheri E. Uniform Trigonometrization Method for Optimal Control Problems with Control Bounds and State Path Constraints. Journal of Spacecraft and Rockets, Accepted 2020;.

[24] Mall K, Taheri E. Optimal Control of Wave Energy Converters Using Epsilon-Trig Regularization Method. In: 2020 Annual American Control Conference (ACC), Accepted; 2020. .

[25] Mall K, Taheri E. Entry Trajectory Optimization for Mars Science Laboratory Class Missions Using Indirect Unified Trigonometrization Method. In: 2020 Annual American Control Conference (ACC), Accepted; 2020. .

[26] Bryson AE. Applied optimal control: optimization, estimation and control. Routledge; 2018.

[27] Taheri E, Junkins JL. Generic smoothing for optimal bang-off-bang spacecraft maneuvers. Journal of Guidance, Control, and Dynamics 2018;41(11):2470–2475.

[28] Patterson MA, Rao AV. GPOPS-II: A MATLAB software for solving multiple-phase optimal control problems using hp-adaptive Gaussian quadrature collocation methods and sparse nonlinear programming. ACM Transactions on Mathematical Software (TOMS) 2014;41(1):1.

[29] Grant MJ, Braun RD. Rapid Indirect Trajectory Optimization for Conceptual Design of Hypersonic Missions. Journal of Spacecraft and Rockets 2014;52(1):177–182.

[30] Aly G, Chan W. Application of a modified quasilinearization technique to totally singular optimal control problems. International Journal of Control 1973;17(4):809–815.

[31] Biegler LT. Nonlinear programming: concepts, algorithms, and applications to chemical processes. Siam; 2010.

[32] Aly G. The computation of optimal singular control. International Journal of Control 1978;28(5):681–688.

[33] Clark CW. Mathematical bioeconomics. In: Mathematical Problems in Biology Springer; 1974.p. 29–45.

[34] Aronna MS, Bonnans JF, Martinon P. A shooting algorithm for optimal control problems with singular arcs. Journal of Optimization Theory and Applications 2013;158(2):419–459.

[35] Luus R. Iterative dynamic programming. Chapman and Hall/CRC; 2000.

[36] Jennings L, Teo K, Fisher M, Goh C, Jennings L, Fisher M. MISER3 version 2, optimal control software, theory and user manual 1997;.

[37] Bressan A. Viscosity solutions of Hamilton-Jacobi equations and optimal control problems (an illustrated tutorial) 2001;.

[38] Luyben WL. Temperature control of continuous stirred-tank reactors by manipulation of fresh feed. Industrial & engineering chemistry research 2004;43(20):6430–6440.

[39] Luus R. Iterative dynamic programming. CRC Press; 2019.

[40] Edgar T, Lapidus L. The computation of optimal singular bang-bang control II. Nonlinear systems. AIChE Journal 1972;18(4):780–785.

[41] Kumar A, Daoutidis P. Nonlinear model reduction and control for high-purity distillation columns. Industrial & engineering chemistry research 2003;42(20):4495–4505.

[42] Yang F, Teo KL, Loxton R, Rehbock V, Li B, Yu C, et al. Visual MISER: An efficient user-friendly visual program for solving optimal control problems. Journal of Industrial and Management Optimization (JIMO) 2016;12:781–810.